Hindawi Publishing Corporation
Journal of Nanomaterials
Volume 2015, Article ID 371582, 5 pages
http://dx.doi.org/10.1155/2015/371582

Research Article

Ferromagnetic Property of Co and Ni Doped TiO_2 Nanoparticles

Qing Wang, Xiaoming Liu, Xuegang Wei, Jianfeng Dai, and Weixue Li

School of Science, Lanzhou University of Technology, Lanzhou 730050, China

Correspondence should be addressed to Qing Wang; wangqing@lut.cn

Received 12 March 2015; Accepted 14 April 2015

Academic Editor: Zijie Yan

The Co and Ni doped diluted magnetic semiconductor nanoparticle TiO_2 is prepared by sol-gel method. $Ti_{0.97}Co_{0.03}O_2$, $Ti_{0.97}Ni_{0.03}O_2$, $Ti_{0.97}Co_{0.06}O_2$, and $Ti_{0.97}Ni_{0.06}O_2$ samples were characterized by X-ray scattering techniques and high resolution transmission electron microscope. The results show that there are no other phases existing in TiO_2. As to the sample of high-concentration dopant, the X-ray scattering techniques have explored the existing of $CoTiO_3$ and $NiTiO_3$. The ferromagnetic measurement shows that the magnetization of the sample of high-concentration dopant increases in the same external magnetic field. However, the relatively higher dopant Co and Ni may form more interstitial ions and paramagnet matters, reducing the oxygen vacancy concentration and finally leading to the decrease of remanent magnetization and coercivity of the materials.

1. Introduction

The diluted magnetic semiconductors (DMS) share the qualities of both semiconductors and magnetic materials, such as ferromagnetism and magnetic and magnetoelectricity. Moreover, the application of the diluted magnetic semiconductors is widely promising in various fields, such as spin light-emitting diode [1], logic device [2], the electric charge of spin valve crystal and spin of electron [3], and nonvolatile memory. As a result, it is one of the hottest research spots and attracts a great number of attentions [4–9].

TiO_2 is a high refractive index transparent and high dielectric constant material. It is also a wide bandgap semiconductor, which can readily generate ferromagnetism when heat treated in vacuum or hydrogen. Since TiO_2 exhibits the characteristics of both the semiconductor and the magnetic material, it can realize the dual control of both electric and magnetic fields by using the electric charge and spin properties of electrons. To achieve the application of the diluted magnetic semiconductors TiO_2, it is important to prepare room-temperature diluted magnetic semiconductor materials with high saturation magnetization intensity. Up to now, the room-temperature ferromagnetism of diluted magnetic semiconductors has been improved by changing the producing method, annealing atmosphere and the appearance of the samples, and doping different metallic ions and nonmetallic ions. Many methods have been used to prepare diluted magnetic semiconductors, such as molecular beam epitaxy (MBE) [10], magnetron sputtering [11], pulsed laser deposition [12], ion implantation [13], and sol-gel method [14]. Different methods have great influence on the properties of material. For example, sol-gel method has the advantages of easy operation and low costs. Moreover, this method can prepare nanoparticles with narrow size distribution and controllable chemical composition at a lower temperature. In this paper, the Co and Ni doped TiO_2 nanoparticles were prepared by the sol-gel method, and the microstructure and ferromagnetism of samples were studied.

2. Experiments

The following is the process of the experiments. Firstly, the 0.057 mol $[CH_3(CH_2)_3O]_4Ti$ is added to anhydrous ethanol (99.9%) with the volume ratio of 1 : 3, and the solution is fully mixed until it converts into the uniform transparent light yellow liquid. Secondly, 622 mg, 1270 mg $Co(NO)_3{\cdot}6H_2O$, 621 mg, and 1268 mg $Ni(NO)_3{\cdot}6H_2O$ are dissolved in 10 mL anhydrous ethanol, respectively. Thirdly, while mixing, 4 mL glacial acetic acid, 2 mL concentrated nitric acid, and 3 mL deionized water are added to the mixed solution, respectively. Fourthly, after the mixed solution is stirred for 4 hours at room temperature, it is aged for 72 hours at room

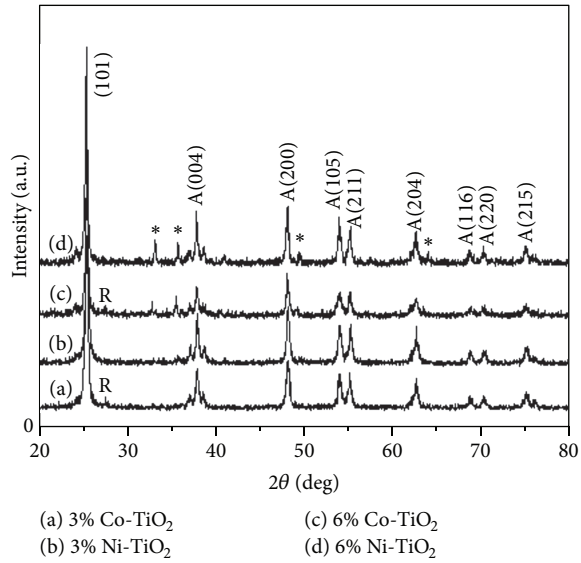

Figure 1: XRD patterns of CN-01, CN-02, CN-03, and CN-04 samples annealed at 500°C for 1 h in the air (A: anatase; R: rutile; and ∗: disturbance phases).

temperature. When the solution converts into stable collosol, the stable collosol is put in the drying oven set at 80°C and dried for 24 hours, by which xerogel is produced. Finally, Markov furnace is used to lay xerogel in the air with an annealing temperature of 500°C to anneal for an hour. After being ground, the nanoparticle TiO_2 is obtained with different concentration and elements. $Ti_{0.97}Co_{0.03}O_2$ (CN-01), $Ti_{0.97}Ni_{0.03}O_2$ (CN-02), $Ti_{0.97}Co_{0.06}O_2$ (CN-03), and $Ti_{0.97}Ni_{0.06}O_2$ (CN-04) are prepared.

3. Results and Discussion

In the present work, the prepared samples were characterized by X-ray diffraction (XRD, D8 advance) with CuKα radiation (λ = 0.15406 nm). Figure 1 is the XRD patterns of Co and Ni doped TiO_2 nanoparticles with different doping concentration. Compared with the standard data (JCPDS, 78-2486), a small amount of rutile is found in the sample of doped Co, while in the sample of doped Ni there is no observation of rutile. The doped 3 mol% sample is pure TiO_2 phase structure, and no other phases were observed, while in the doped 6 mol% sample there are disturbance phases, which are produced mainly due to high dosage concentration. Moreover, from Figure 1, it is observed that the diffraction peaks of Ni doped sample are sharper and stronger than Co doped samples, so that the crystallinity of Ni doped TiO_2 is more superior than that of Co doped sample. By comparing 3 mol% Co doped sample with 6 mol% Co doped sample, it is found that there is no obvious change of diffraction angle, and the only difference is that the diffraction peak of Co doped 3 mol% is stronger, which means superfluous doped Co will decrease the crystallinity. As for the doped Ni, the diffraction peak of doped 3 mol% Ni is stronger than that of doped 6 mol% Ni. By using the Scherrer equation $D = 0.9\lambda/\beta\cos\theta$ and taking (101) crystal face diffraction peak as standard, it is calculated that the sizes of doped 3 mol% Co grain and doped 3 mol% Ni grain are 29.71 nm and 34.15 nm, respectively.

High Resolution Transmission Electron Microscopy (HRTEM, JEM-2010) is used to observe the microstructure of the sample and the change of the interplanar spacing between doped samples. Figure 2 shows the results of HRTEM observation of samples CN-01 and CN-02. Figure 2(a) shows that the sizes of the prepared nanoparticles are between 30 and 40 nm, and the images of their corresponding electron diffraction rings are inserted below. The diffraction ring of the nanoparticles is presented as a spotty ring micrograph, and there are no other phases of diffraction spots such as Co, CoO, Co_3O_4, $CoTiO_3$, or $CoTi_2O_5$. This means that no structure change of anatase TiO_2 was found. According to the standard electron diffraction ring data (JCPD, 78-2486), the corresponding crystal face of the diffraction ring can be judged; they are (101), (103), (200), and (105) from outside to inside.

Figure 2(b) is the corresponding lattice structure. In the figure, there is no extra lattice imperfection; on the contrary, the observation shows that there are many regularly arranged wrinkled stripes, which means they have high crystallisation degree. The interplanar spacing is 0.3533 nm, and its corresponding crystal face (101) is slightly increased compared with the standard micrograph (JCPDS, 78-2486), which is caused by lattice distortion. Thus, it is proved again that Co^{2+} replaces Ti^{2+} in the lattice of TiO_2. Figure 2(c) is the appearance of the sample of doped Ni. As the figures show, the shape of nanoparticles is block, and the sizes are between 10 nm and 40 nm. The pictures of their corresponding electron diffraction rings are inserted below, and the diffraction ring of the nanoparticles is also presented as a spotty ring micrograph. In Figure 2(d), it is measured that the corresponding interplanar spacing of crystal face is 0.3528, which means Ni^{2+} replaces Ti^{2+}.

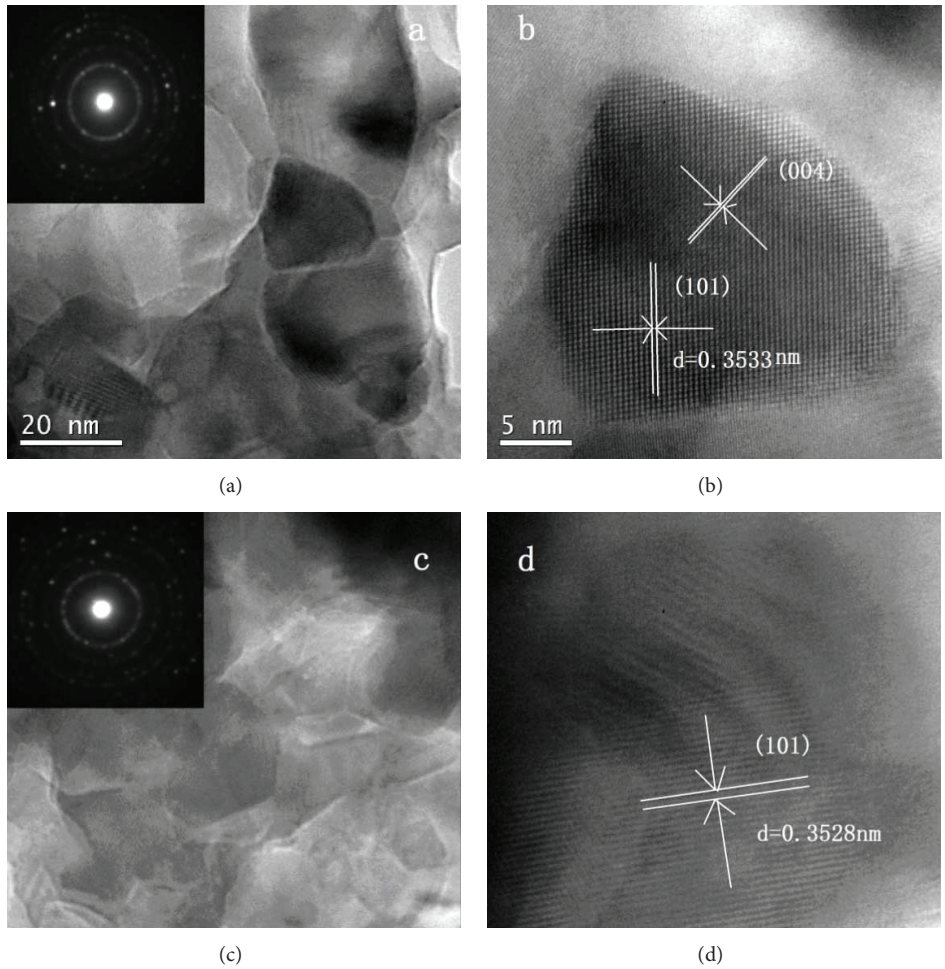

Figure 2: (a–d) display the HRTEM micrographs: (a, b) CN-01; (c, d) CN-03.

Figures 3(a) and 3(b) are the EDS (Genesis XM2) spectra of the samples CN-01 and CN-03, respectively. The figures show except the samples come from the characteristic peak (8.1 and 8.9 Kev) of Cu in the bronze grating which carry the samples in the experiment; in the samples, there are only O, Ti, Co (CN-01) and O, Ti, Ni (CN-03) three elements. In Figure 3(a), the atom percentages of O, Ti, and Co are 65.22, 33.81, and 0.97, respectively, while in Figure 3(b), the percentages are 65.02, 33.96, and 1.02. The results show that, in the doped samples, there are only doped elements, and the percentage of the doped elements is close to the doped 3 mol% in the experiment.

The magnetic properties were investigated by a vibrating sample magnetometer (VSM 7403, Lakeshore, USA). Figure 4 is the magnetic hysteresis loops of the four samples tested at 300 K. The figure shows that all the samples are magnetic at room temperature. In Figure 4(a), in the relatively weak applied magnetic field, the intensity of magnetization of the sample CN-02 reaches its saturation condition, while the intensity of magnetization produced by sample CN-01 is stronger than that of sample CN-02. Moreover, in the applied magnetic field, the intensity of magnetization sample CN-01 does not reach its saturation condition at 2000 (Oe). The illustrations are residual magnetization (Mr) and coercivity (H) of sample CN-01 and sample CN-02 measured at room temperature, from which the residual magnetization produced by sample CN-01 is higher than that of sample CN-02, but it is evident that its coercivity is lower than sample CN-02. It proves that magnetism produced by the samples is relevant to Co^{2+} and Ni^{2+} themselves.

Figure 4(b) is the magnetic hysteresis loops of samples CN-03 and CN-04. The figure shows that hysteresis produced by the samples has not reached the saturation condition, the quality of which also exists in the nanoribbon or nanoparticles of TiO_2 doped with Co^{2+} or Ni^{2+} [13, 14]. After comparing the samples CN-01 and CN-02, the intensity of magnetization produced by samples CN-03 and CN-04 increases to different extent, but the residual magnetization (Mr) and coercivity (H) are apparently decreased, as is shown in Table 1. The major reason is that, with the increase of dosage concentration, more doping ion Co^{2+} or Ni^{2+} replaces Ti^{4+} in the samples which increase the intensity of magnetization produced by the samples. The reason why the residual magnetization (Mr) and coercivity (H) produced by them are apparently decreased is that the high dosage concentration

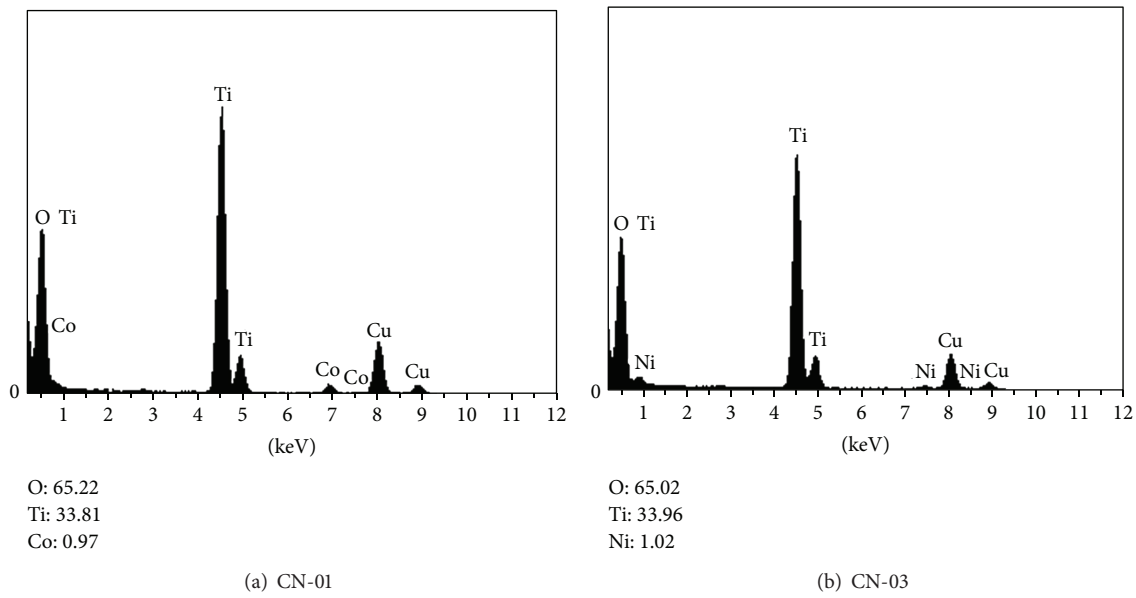

Figure 3: EDS spectra of 3 mol% doped TiO_2 samples. (a) CN-01. (b) CN-03.

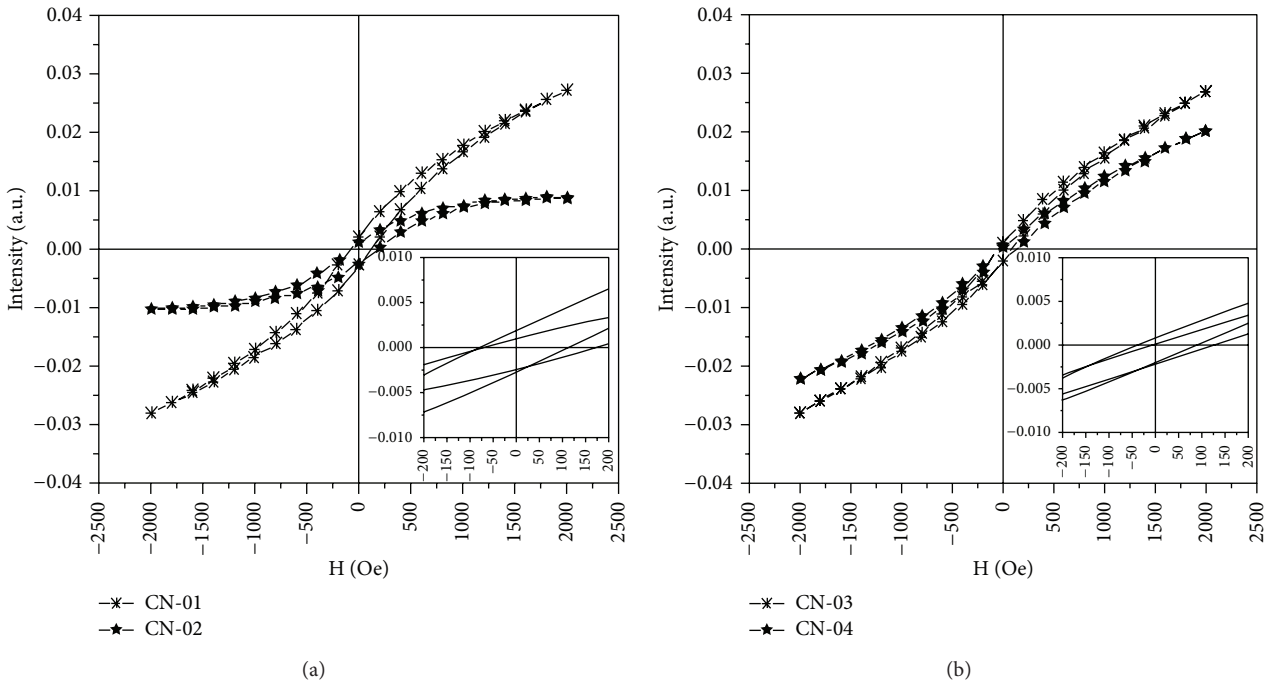

Figure 4: The magnetic hysteresis loops measured at room temperature for the CN-01, CN-02, CN-03, CN-04 samples.

produces paramagnetic phases $TiCoO_3$ and $TiNiO_3$ in the growing process of crystal. Moreover, in Figures 4(a) and 4(b), the intensity of magnetization produced by Co^{2+} doped TiO_2 is greater than Ni^{2+}. Since there exist differences in orbital electron number of Co^{2+} and Ni^{2+}3d, it is certain that the room-temperature ferromagnetism produced by the samples has relevance with the orbital electron of doped Co^{2+} and Ni^{2+}3d, not from the defects of the samples themselves.

It is still not clear about the origin of DMS ferromagnetism. There are currently two theories to explain the observed ferromagnetism. One is the ferromagnetic exchange coupling mediated by carriers, and the other is the bound magnetic polaron (BMP) model, which is related to the defects in materials. The above study means that the origin of DMS ferromagnetism is due to the carriers exchange coupling.

Table 1: The Ms, Hc, and Mr parameters of samples CN-01, CN-02, CN-03, and CN-04.

Sample	Ms (emu/g)	Hc (Oe)	Mr (emu/g)
6 mol% Co	0.027	88.6	0.0009
6 mol% Ni	0.020	132.9	0.0003
3 mol% Co	0.027	115.2	0.0021
3 mol% Ni	0.008	181.7	0.0011

4. Conclusions

By using the sol-gel method, the diluted magnetic semiconductor nanoparticle Co and Ni doped TiO_2 is produced with the concentration of 3 mol% and 6 mol%. The research results show that firstly Co^{2+} doped samples CN-01 and CN-03 produce the phase of rutile, while in the same condition, Ni^{2+} doped samples CN-02 and CN-04 belong to anatase structure and there is no rutile phase. Moreover, the XRD peak of Ni^{2+} doped samples is stronger than Co^{2+} doped samples of the same concentration. Secondly, the differences of electronic states of Co^{2+} and Ni^{2+} influence the growth patterns of the samples: Co^{2+} doped samples grow spherically and Ni^{2+} doped samples grow massively. Finally, the diluted magnetic semiconductor nanoparticles TiO_2 doped by metal ion and room-temperature ferromagnetism have relevance with doped cations themselves which mainly rely on the interaction between the doped cations and 3D orbital electron.

Conflict of Interests

The authors declare that there is no conflict of interests regarding the publication of this paper.

References

[1] G. Kioseoglou and A. Petrou, "Spin light emitting diodes," *Journal of Low Temperature Physics*, vol. 169, no. 5-6, pp. 324–337, 2012.

[2] D. A. Allwood, G. Xiong, C. C. Faulkner, D. Atkinson, D. Petit, and R. P. Cowburn, "Magnetic domain-wall logic," *Science*, vol. 309, no. 5741, pp. 1688–1692, 2005.

[3] M. Hafeez, A. Ali, S. Manzoor, and A. S. Bhatti, "Anomalous optical and magnetic behavior of multi-phase Mn doped Zn_2SiO_4 nanowires: a new class of dilute magnetic semiconductors," *Nanoscale*, vol. 6, no. 24, pp. 14845–14855, 2014.

[4] S. Mehraj, M. S. Ansari, and Alimuddin, "Structural, electrical and magnetic properties of (Fe, Co) co-doped SnO_2 diluted magnetic semiconductor nanostructures," *Physica E: Low-Dimensional Systems and Nanostructures*, vol. 65, pp. 84–92, 2015.

[5] D. Yao, X. Zhou, and S. Ge, "Raman scattering and room temperature ferromagnetism in Co-doped $SrTiO_3$ particles," *Applied Surface Science*, vol. 257, no. 22, pp. 9233–9236, 2011.

[6] N. Bahadur, R. Pasricha, S. Chand, and R. K. Kotnala, "Effect of Ni doping on the microstructure and high Curie temperature ferromagnetism in sol-gel derived titania powders," *Materials Chemistry and Physics*, vol. 133, no. 1, pp. 471–479, 2012.

[7] Y.-B. Sun, X.-Q. Zhang, G.-K. Li, and Z.-H. Cheng, "Effects of oxygen vacancy location on the electronic structure and spin density of Co-doped rutile TiO_2 dilute magnetic semiconductors," *Chinese Physics B*, vol. 21, no. 4, Article ID 047503, 2012.

[8] P. Varshney, G. Srinet, and R. Kumar, "Room temperature ferromagnetism in sol-gel prepared Co-doped ZnO materials," *Science in Semiconductor Processing*, vol. 15, pp. 314–319, 2012.

[9] G. Drera, M. C. Mozzati, P. Galinetto et al., "Enhancement of room temperature ferromagnetism in N-doped TiO_{2-x} rutile: correlation with the local electronic properties," *Applied Physics Letters*, vol. 97, no. 1, Article ID 012506, 2010.

[10] S. A. Chambers and T. Droubay, "Clusters and magnetism in epitaxial Co-doped TiO_2 anatase," *Applied Physics Letters*, vol. 82, no. 8, pp. 1257–1259, 2003.

[11] K. A. Griffin, A. B. Pakhomov, C. M. Wang, S. M. Heald, and K. M. Krishnan, "Cobalt-doped anatase TiO_2: a room temperature dilute magnetic dielectric material," *Journal of Applied Physics*, vol. 97, no. 10, pp. D320–D322, 2005.

[12] H. H. Nguyen, W. Prellier, J. Sakai, and A. Ruyter, "Substrate effects on the room-temperature ferromagnetism in Co-doped TiO_2 thin films grown by pulsed laser deposition," *Journal of Applied Physics*, vol. 95, no. 11, pp. 7378–7380, 2004.

[13] C. M. Wang, V. Shutthanandan, S. Thevuthasan, T. Droubay, and S. A. Chambers, "Microstructure of Co-doped TiO_2 (110) rutile by ion implantation," *Journal of Applied Physics*, vol. 97, no. 7, Article ID 073502, 2005.

[14] R. Suryanarayanan, V. M. Naik, P. Kharel, P. Talagala, and R. Naik, "Ferromagnetism at 300 K in spin-coated films of Co doped anatase and rutile-TiO_2," *Solid State Communications*, vol. 133, no. 7, pp. 439–443, 2005.